Journal of Materials and Environmental Science
ISSN : 2028-2508
e-ISSN : 2737-890X
CODEN : JMESCN

J. Mater. Environ. Sci., 2022, Volume 13, Issue 09, Page 1101-1116

http://www.jmaterenvironsci.com

Geo-environmental Study of Geomorphological and Geological Features of Parts of Benue Trough using Advanced Space-borne Thermal Emission and Reflection Radiometer (ASTER) data

I.A. Omenikolo[1, 2] *, A.I. Opara [2], C.N. Okereke[2], D.O. Ikoro[2], I.A. Oha[3], T.T. Emberga[1], C. C. Agoha[2], G.E. Inyang[2], and C.N. Nwokeabia[4]

[1] Department of Physics/Electronics, Federal Polytechnic Nekede, P.M.B. 1036, Owerri, Nigeria.
[2]Department of Geology, Federal University of Technology, P.M.B. 1526 Owerri, Nigeria.
[3] Department of Geology, University of Nigeria, Nsukka. Nigeria.
[4]Department of Applied Geophysics, Nnamdi Azikwe University Awka, Nigeria.
**Corresponding author, Email address: omenikoloalexander@gmail.com*

Received 02 Sept 2022,
Revised 29 Sept 2022,
Accepted 30 Sept 2022

Keywords
- ✓ ASTER
- ✓ Lineaments,
- ✓ Lineament density,
- ✓ Band ratio colour (BRC),
- ✓ False colour composite.

omenikoloalexander@gmail.com
Phone: +2348055820383

Abstract

The structural Interpretation over parts of Benue Trough using Advanced Space-borne Thermal Emission and Reflection Radiometer (ASTER) data, was carried out to depict structural complexity related to the basin, analyzing lineaments to deduce the economic potentials of the study area. The processing and analysis of the ASTER imagery were carried out using ArcGIS V10.5 and ERDAS IMAGINE 2015 software by applying several digital image enhancement techniques such as general contrast stretching, edge enhancement, Band ratio colour combination images, and False-colour composite, to provide suitable knowledge about the geology, lithology and the prevalent minerals. Three False colour composite images, RGB 321, RGB 468, and RGB 742 were generated and used to interpret geological structures. Band Ratio of 4/2 revealed areas where iron minerals are abundant, especially around Abakaliki, Ankpa, and Oturkpo. Linear features with trend directions of E – W, NW – SE, and NE – SW with dominant orientation in the NE – SW were also interpreted from the study area. Lineament density analysis revealed areas with very high, high, moderate, low, and very low lineament densities with values of 47,500m^2, 35,000m^2, 25,000m^2, 15,000m^2, and 5,000m^2 respectively. These lineaments are believed to have controlled mineralization across the study area.

1. Introduction

The application of remote sensing data in the interpretation of linear features and other geological structures has recently increased and efficiently become a very useful advancement in the geological investigation. Structural and geological mapping is generally carried out using remote sensing technique [1,2]. The effectiveness of this technique is more pronounced when it is combined with complementary data like geophysical data. This past decade has witnessed a shift of the technique from its primary application to mapping of structures, detailed interpretation of sedimentary structures, lithological variation, and structural kinematic analysis [3]. Remote sensing can extract a multitude of data about the structure and composition of the Earth's

surface using satellite image acquisition and interpretation processes. Lineament mapping exhibits a major function in geological interpretation, particularly during mining, mineral, and hydrocarbon exploitation. Most of the geological investigations employ completely a thorough understanding of the subsurface geological and lineament knowledge since they are often related to mineral location and tectonic trend [4]. Several studies have been carried out based on geophysical investigations to delineate the structural patterns and tectonic framework within the Benue Trough [5,6,7,8,9,10,11-19]. The study of geological structures like lineaments, which may appear as fractures, joints, and faults are of great importance since they are zones for ores, minerals, water reservoirs, and also harbor hydrocarbon [20,21]. Magowe and Carr [22] defined lineament as surface expressions having fractures, joints, and other straight /curvilinear structures occurring on and below the earth's surface. Concerning the properties of remote sensing data, Moawad [23] pointed out lineaments as a set of pixels having identical discrete numbers. The early set of remote sensing data was reported by [24], that lineament extraction was initially seen light table, transparent and stereo pair. According to [25], identification of lineaments on remote sensing data describes weak geological zones on the surface of the earth and represents traces of fracture. The processing and analysis of remote sensing images involve the delineation of lineament having different wavelength intervals [26]. Opara et al. [27] studied the characteristics of structures in parts of Benin Basin using Landsat and aeromagnetic data, meso-fracture zone, and linear structures observed having major trends in the NE-SW and N-S directions. Pournamdari et al. [28] carried out lithological mapping in Iran by employing Landsat 5 TM and Terra ASTER using transformation techniques such as Band Ratio, Correlation Coefficient, Optimum Index Factor, and Principal Component Analysis (PCA). The result showed the use of ASTER data to develop RGB Band ratio of (4/1,4/5,4/7) for discriminating lithological units in the study area. The Correlation Coefficient and Optimum Index Factor exhibited a nice correlation with the geology map. Gad and Kusky [29] employed the mapping of lithology in the Arabian–Nubian shield, Sinai, Egypt using ASTER Band ratio of (4/7, 4/6, 4/10). The result revealed that the band ratio is appropriate for mapping the rock units which include volcanogenic sediment, amphibolite, migmatite, gneiss, and banded iron formation. The different procedures involved in the delineation of lineament from remote sensing data include enhancement and lineament extraction methods. The methods are vital for the analysis and extraction of lineaments to decipher areas connected with hydrocarbon potentials. Digital Elevation Model (DEM) and remote sensing data can be employed in delineating lineaments through aligning of features. The features are vegetation, soil moisture, and topography, which can be investigated using texture, pattern, tone, colour, and topography attributes [30]. ASTER is a multispectral imager launched in December 1999. It covers the region of the electromagnetic spectrum using fourteen (14) bands, from visible to thermal infrared regions with different resolutions. It covers 3 bands in the visible near-infrared having a resolution of 15 m, also 6 bands in the short-wave infrared having a resolution of 30 m, and then 5 bands in thermal Infrared having a resolution of 90 m. The sensor provides a favorable success in extracting Digital Elevation Models (DEM). ASTER scene covers an area of 60 x 60 km. Several studies have been carried out ASTER data for geological interpretation [31,32,33,34,35,36,37]. This study, therefore, presents the structural investigation using ASTER data with the objectives of depicting lineaments, mapping landforms, and their structural orientation and identifying the dominant trend of the most remarkable tectonic events to make inferences about the mineralization potentials of the study area.

2. The geology of the study area

The Benue trough is an important rift system in Africa and forms a feature of considerable structural significance in Nigerian geology. It has an extension from the Niger Delta through the Gongola Rift to the Chad Basin in the north. It trends in the direction N-E, having a width of about 130-150km with an approximated length of 800km. The Benue trough is occupied by cretaceous rocks with age ranging from middle Albian to Maestrichtian and bordered on each side by gneisses and granites of Proterozoic age making the crystalline basement. It is a NE-SW trending sedimentary basin, whose development has been very closely associated with the separation of Africa from South America and the opening of the Atlantic Ocean [38,39,40,41,42]. In the early theory of the origin of Benue Trough, [43] proposed that the trough came into existence as a rift structure related to stress and subsequently the separation of Africa and South America.

The trough is grouped into the Lower, Middle, and Upper Benue regions based on stratigraphic and tectonic considerations. Figure 1 is the geologic map showing the study area.

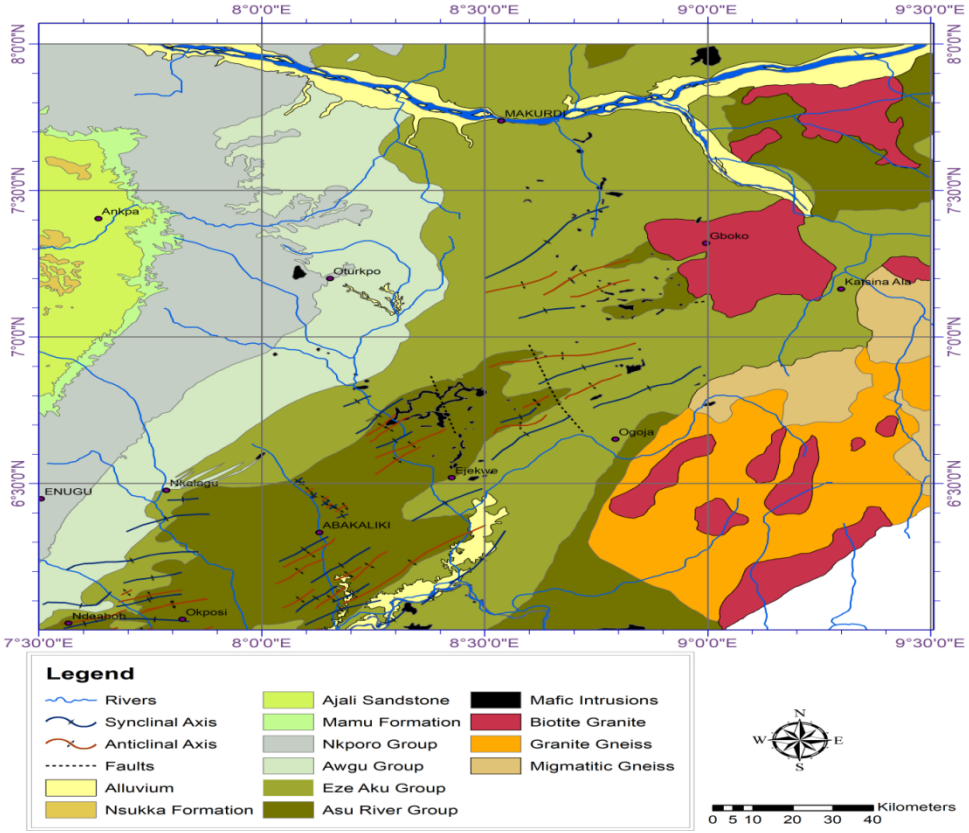

Figure 1. Geologic map of the study area showing the structural elements

The area is distinguished by thick sedimentary cover of different formations within the age range between Albian to Maastrichtian, the earliest being the Asu-River group of the Albian age [44]. Asu-River Group is the oldest sedimentary section deposited in the basement of the Benue Trough [45]. It consists of shales, limestones, sandstones, and siltstones. This was followed by Ezeaku Formation during the Turonian regression period and comprised of argillite, with occasional beds of limestone, carbonate, and shale. Others include Keana/Awe Formation, Awgu Formation, and Lafia sandstone as the youngest sediment [44]. The event of stages of deposition in the Benue Trough is distinguished by periods of marine regression and transgression [46,47]. A Series of tectonic activities affected the sedimentary sequences in the trough, resulting in two stages, the Cenomanian and the Santonian deformations [48,49]. The Santonian was distinguished by a series of compressional folding, trending in the NE-SW orientation and parallel to the trough edge. The emergence of Abakaliki Anticlinorium was affected as a result of folding episode which occurred during the Santonian deformation.

3. *Materials and Method*

The study area is located in the Benue Trough, Nigeria within latitude 6° 00^{1}N to 8° 00^{1}N and Longitude 7° 30^{1}E to 9° 30^{1}E. It covers an aerial extent of approximately 175,561km^{2}. Space-borne multispectral images offer considerable advantages in the conduct of regional geologic mapping and mineral exploration. These datasets present clues that lead to the generation of information relating to lithologic discrimination, structural feature extraction, and hydrothermal alteration. The ASTER data was downloaded via the NASA Earth Data platform. It consists of 36 free cloud 1T ASTER 003 version imagery that covers part of the study. A 60km x 60km multispectral scene was obtained between 25th January 2001 and 7th February 2008. ASTER as a multispectral device is made up of 14 bands, comprising three (3) bands in the visible and near-infrared (VNIR), six (6) bands

in the shortwave Infrared (SWIR), and five (5) bands in the thermal infrared (TIR), with spatial resolution in the order fifteen (15), thirty (30) and ninety (90) meters respectively. The characteristics of ASTER data are given in Table 1. As a result of its enhanced and better spatial resolution particularly within the visible and near-infrared, ASTER Band ratios and Colour composites are applicable for structural and geologic mapping. The Advanced Spaceborne Thermal Emission and Reflection Radiometer (ASTER) data covering the area of interest were prepared for digital image processing using ERDAS, ENVI, and PCI image processing software. Digital elevation models (DEMs) are a representation of the earth's geomorphology and are useful in delineating structural information on the earth's surface. Digital Elevation Model was downloaded to study and identify the elevation differences and the lineament features within the study area. This was carried out by searching in the Global Land Cover Facility search for the map area by inserting the latitude and longitude coordinates and SRTM (Shuttle Radar Topographic Mission) was selected, acquired, and used for the intended analysis.

3.1 Pre-processing of satellite images

Before using the satellite images, it is necessary to compensate for different inherent errors. The techniques applied to compensate and correct errors and distortions in the images are pre-processing. The preprocessing phase of ASTER data involves those operations that are needed before the main data extraction and analysis of information. These operations are usually classified as geometric and radiometric corrections. Geometric correction takes into consideration the geometric errors in the data acquisition system and records the satellite image to a map projection. Radiometric correction is the correction of radiometric errors due to sensor-specific errors and to the atmospheric condition during recording. For many applications, the corrected image is also treated by different image enhancement techniques to improve the quality and facilitate the analysis.

Table 1. ASTER Data Characteristics (Modified after [50])

Radiometric	Ground Resolution	Spectral Region	Spectral range (μm)	Band Number
8 bits	15 m	VNIR	0.52–0.60 0.63–0.69 0.78–0.86 0.78–0.86	Band 1 Band 2 Band 3-N Band 3-B
	30 m	SWIR	1.60–1.70 2.145–2.185 2.185–2.225 2.235–2.285 2.295–2.365 2.360–2.430	Band 4 Band 5 Band 6 Band 7 Band 8
12 bits	90 m	TIR	8.125–8.475 8.475–8.825 8.925–9.275 10.25–10.95 10.95–11.65	Band 10 Band 11 Band 12 Band 13 Band 14

The image processing techniques including False Colour Composite (FCC), Band Rationing, and Normalized Vegetation Index image were applied to the data to determine the desired information and facilitate the discrimination of lithological units and geological feature.

3.2 False Colour Composite (FCC)

A False Colour Composite (FCC) image is an effective means for the visual interpretation of multi-spectral imagery. They are effective in highlighting different features on the Earth's surface, and very useful for remote sensing studies. False-colour composite permits the visualization of wavelengths that the human eye cannot see (i.e. near-infrared and beyond). With the assistance of bands like near-infrared that display the spectral differences and often increase data interpretation. The selection of colours from multispectral imagery is carried

out in an arbitrary process. As a result of this, the colour of a target in the image displayed does not depict or exhibit any similarity to its natural colour. Therefore, the outcome of the product is referred to as a false colour composite image. Series of procedures can be adopted in the production of false colour composite images. However, possible procedures may be more appropriate for revealing certain objects in the image.

3.3 Band Rationing

Band rationing is a technique used to enhance the spectral differences between bands and reduce the shadow effects caused by topography. It is an enhancement process in which the DN(Digital Number) value of one band is divided by the DN value of another band. Therefore, if the values are related, the resultant division is a number close to 1. But if the value of the numerator is less than the value of the denominator, the result will approach zero. If this is reversed, the result will be well above 1 [19]. Band ratios can be useful for highlighting certain features or materials that cannot be seen in the raw bands [51]. A ratio of ASTER band l over band 2 will either enhance the small contribution of iron oxide minerals or will discriminate it in the study area. The ratio of 2/1 is useful for mapping iron oxides because it has an absorption in the blue region and high reflectance in the red region.

3.4 Normalized Difference Vegetation Index (NDVI)

Normalized Difference Vegetation Index (NDVI) is a pointer or an index employed in quantifying vegetation and also has beneficial use in knowing vegetation density and evaluating the variations in plant health. Indices of vegetation depend on the observation that separate surfaces reflect different classes of light separately. Photo synthetically, most vegetation that is active absorbs the red lights that fall on it and reflects most of the near-infrared band. Whereas dead or inactive vegetation reflects red light more than near-infrared light. Also surfaces without vegetation exhibits more reflectance through the light spectrum. The index of vegetation can be defined by taking the ratio of red and near-infrared bands. The most frequent of these ratio indices for vegetation is probably the Normalized Difference Vegetation Index. The normalized difference vegetation index (NDVI), is the ratio of the difference between the near-infrared band (NIR) and the red band (R) and the sum of these two bands (equation 1).

$$\mathrm{NDVI} = \frac{\mathrm{NIR}-\mathrm{RED}}{\mathrm{NIR}+\mathrm{RED}} \qquad \text{Eqn. 1}$$

Where NIR is the reflectance in the near-infrared band and RED is the reflectance in the visible red band. Normalized Difference Vegetation Index (NDVI) can be estimated for any image comprising red and near-infrared bands. The output of NDVI (figure 4) is a measure of the vegetation richness of an area. NDVI values range from -1 to +1, and values that are less than zero lack ecological meaning. Therefore, the index range is round down from 0 to +1. This implies that high values indicate a large difference between the red and near-infrared radiation registered revealing active photosynthetic vegetation. While low values imply a small difference between the red and NIR signals, revealing little photosynthetic activity.

4. Results and Discussion

4.1 Results

The Advanced Spaceborne Thermal Emission and Reflection Radiometer (ASTER) images were processed to interpret geological studies of the study area. Digital techniques involving linear enhancement, and image classification, were employed to enhance linear features, and interpret the lithological units and geological structures. Through image processing, drainage patterns, fractures/lineaments, and geological maps were generated. Figure 2 shows the lineament superimposed on the drainage map of the study area. The drainage pattern is dendritic which is indicative of lithological, structural, and topographic differences. It is also indicative of alluvial rocks, which is typical of the geology of the area that consists mainly of sedimentary rocks. The drainage texture of the area is variable (coarse to fine). The dendritic feature implies that underlying sediment is a homogenous unit. Also, the pattern may indicate that the lithology possesses the least resistance to the erosive action of the streams and rivers. The lithological unit includes clay, mudstone, shale, and limestone. The

dendritic pattern is observed in some parts of the study area, Makurdi, Katsina-ala, and Otukpor interpreted as regions having sediments arranged horizontally or uniformly crystalline rocks.

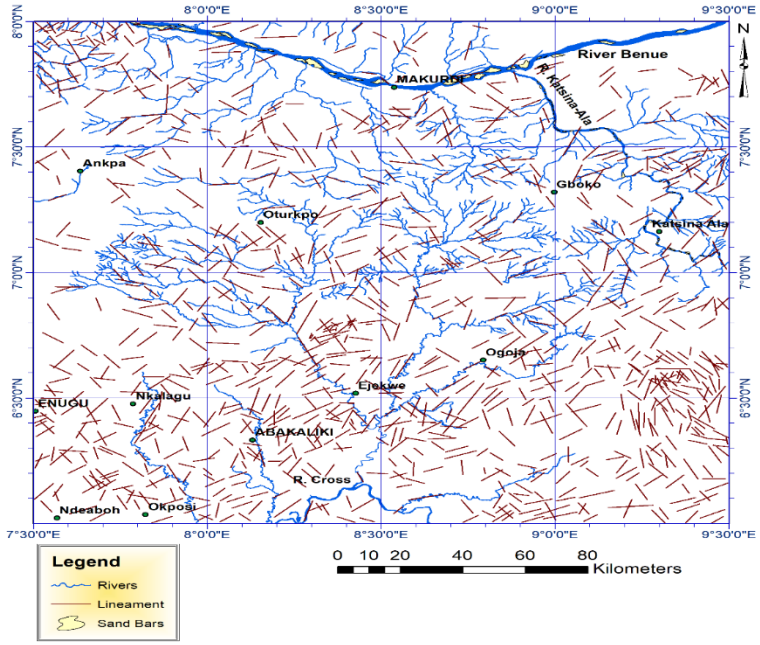

Figure 2: Lineament on Drainage map

Figure 3 is the Digital elevation model (DEM) for the study area. It reveals a peak value of 1900m and the lowest value of 0m. From the elevation model, some regions like Ankpa, Enugu, Oturkpo, Gboko, and katsina Ala have the highest elevation while areas like Nkalagu, Abakiliki, Ejekwe, and Ogoja have the lowest elevation. Figure 4 is the Normalized Difference Vegetation Index map of the study area. It was produced to depict regions of bare rocks and vegetation.

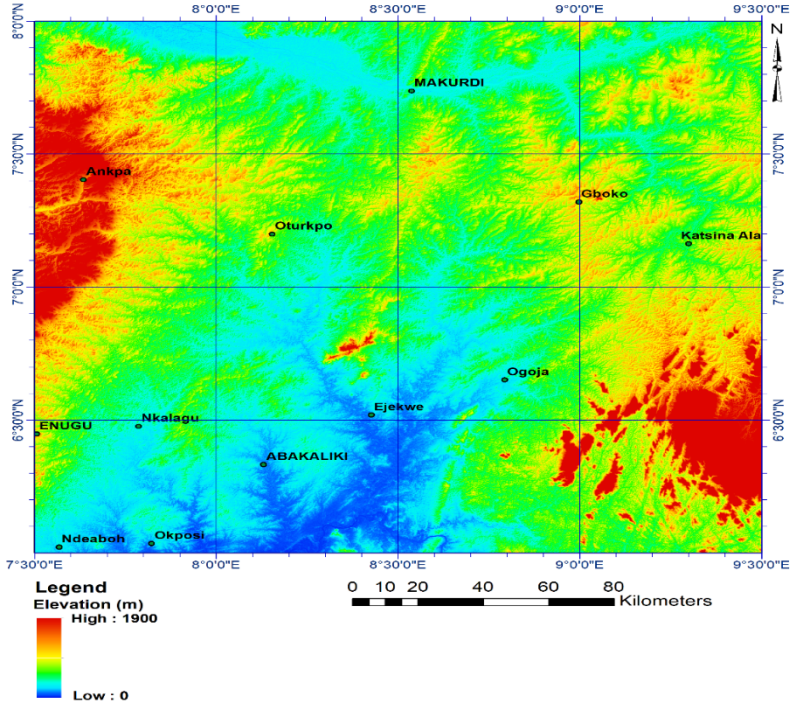

Figure 3: Digital Elevation Model (DEM) of the study area

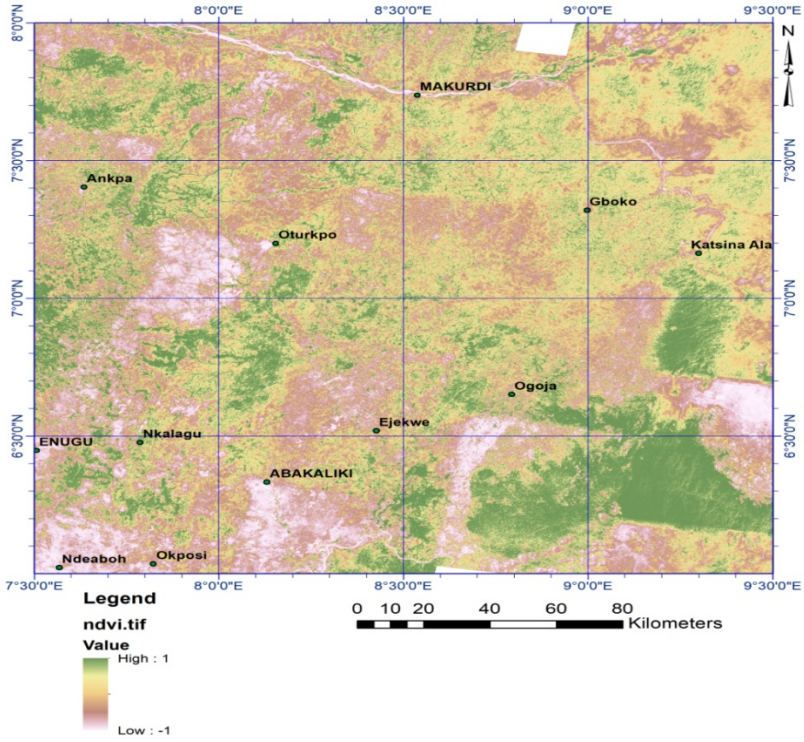

Figure 4: Normalized Difference Vegetation Index (NDVI) map of the study area

The healthier plants possess high values of NDVI as a result of high reflectance of infrared and low reflectance of red light. The NDVI revealed that the dark brown region corresponds to bare rock areas which are observed around Ogoja, Ejekwa. Light brown areas correspond to soil plus little vegetation and are observed around Ndeaboh, Okposi, and Abakaliki which corresponded with the exposure of the Azu River group. However, intense green patches suggesting thick vegetative cover were observed. A total of 983 lineaments were identified and delineated to generate a lineament map for the study area. Linear features equal to or more than 1000m of length were applied. The extracted lineament from ASTER data, exhibited two distinct sets of linear structures in the NW-SE and NE-SW, having the NE-SW direction as the dominant structural trend. Umeji [52], recognized Pan African Orogeny as distinguished by NNE-SSW to NNW-SSE trend structures with a varying amount of intrusive, while the lower Cretaceous area of Nigeria Is distinguished by NE-SW shear zone orientation and fractures influenced by volcanism. The interpreted lineament of the study area is presented as a lineament map and lineament density map respectively (Figures 5 & 6). The study area showed traces of lineaments observed in areas with basement outcrops nearer to the surface. The lineament trends corresponded to the position and direction of the paleo-tectonic fracture zones of the study area, which includes the St Paul's and Romanche Fracture Zones. The lineaments with longer lateral extension revealed trends in the NE-SW, which is an indication of the direction of the last regional tectonic phase.

It is also observed that some lineaments in this area run parallel to each other and cross-cut each other simultaneously, exhibiting a conjugate system associated with wrench tectonics. Therefore, this shows that the fracture and fault are evidence of transpressional, trans-tensional, and extensional movements along oceanic fracture zones as African and South American Plates separated [53,54]. This is an indication that this region has witnessed intense tectonic activities. It also implies that the areas are sedimentary and magnetic basement contacts [55].

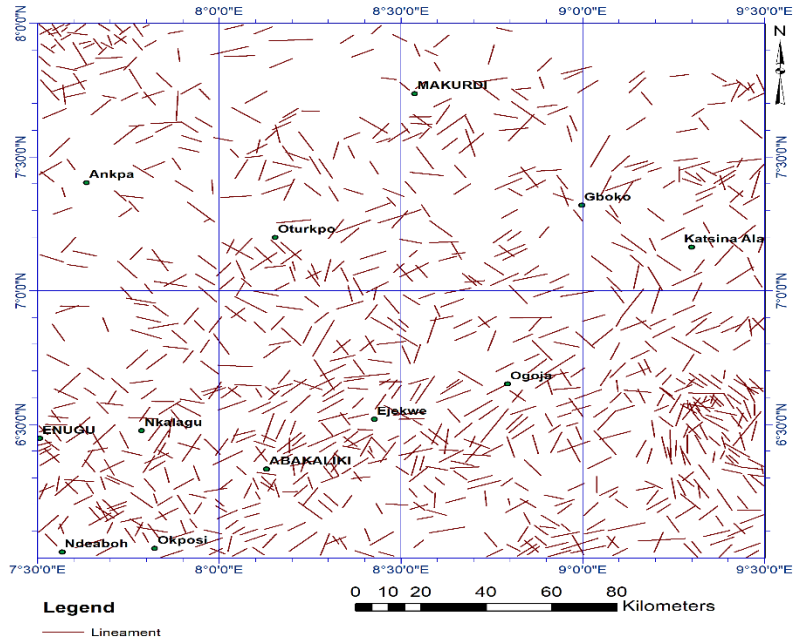

Figure 5: Lineament Map

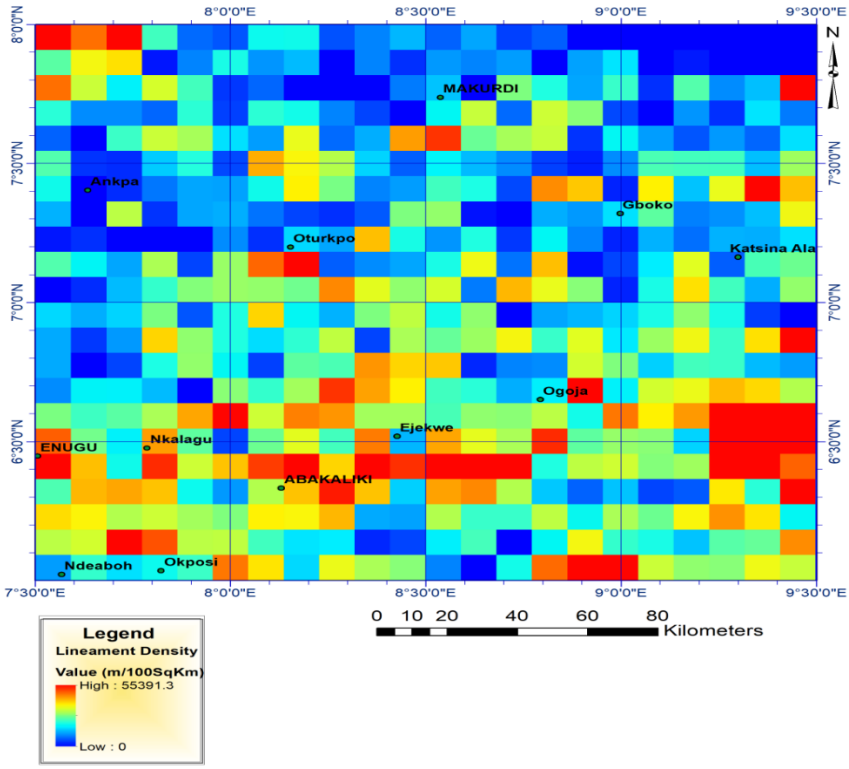

Figure 6: Lineament Density Map

The analysis of the lineament density is aimed at calculating the frequency of lineament per unit area. This deduction is utilized in producing a map that reveals the rate of concentration of the lineament within the grid cell. The lineament density map in Figure 5, reveals a high concentration of lineaments around Enugu, Nkalagu, and Abakaliki. This suggests that these areas are sites of intense tectonic/magmatic activities and may therefore be strongly deformed. The map of lineament density, revealed areas having very high, high, moderate, low and very low lineament densities identified as 47,500m^2, 35,000m^2, 25,000m^2, 15,000m^2 and 5,000m^2 which represent 37.25%, 27.45%, 19.60%, 11.76% and 3.92% respectively. Table 2 shows the lineament density classification. Lineament quantification and statistical analysis were carried out with particular reference to the

orientation of the lineaments. This was done to prepare a rose diagram with established structural trends (Figure 7). Rose diagrams were plotted using visually extracted lineaments with the lengths of the rosette blades proportional to the square of the relative frequencies of the lineaments. The rose diagram revealed lineament trend directions of E – W, N – S, NW – SE, and NE – SW having the dominant orientation in the NE – SW direction which is similar to the major lineament trend of the study area. The E-W, NW-SE, and N-S, depict the older and deeper tectonic directions. The NE-SW direction depicts the younger tectonic event, this is because the younger event predominantly obliterates the older event.

Table 2: Classification of lineament density of the study area

Classification	Area (m^2)	Average Area (m^2)	Percentage (%)
Very low lineament density	0 -10,000	5,000	3.92
Low lineament density	10,000 - 20,000	15,000	11.76
Moderate lineament density	20,000 - 30,000	25,000	19.60
High lineament density	30,000 - 40,000	35,000	27.45
Very high lineament density	40,000 - 55,000	47,500	37.25
Total		127,500	99.98 ≈100

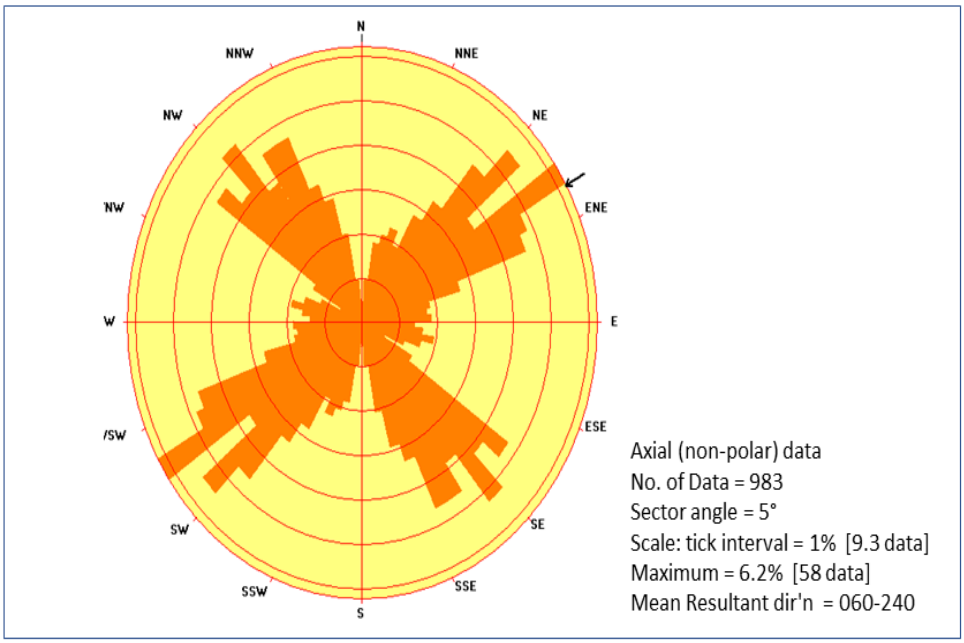

Figure 7: Rose diagram of the Study area

The colour composite was produced to enhance spectral signatures of the images in the study area, thus improving the observation of the different patterns which can be attributed to the various stratigraphic units existing in the area. This study presents the following three (3) false colour images, RGB 321, RGB 468, and RGB 742 (Figures 8, 9, and 10) respectively were generated and used to interpret geological structures and distinguish them from other land surface materials. The false colour combination of the study area indicates that some areas are green in colour showing the presence of vegetation, while brownish areas are possibly non-vegetated areas and the bluish areas show typical water bodies. The major advantage of this composite is its ability to discriminate (broadly) between different lithologic groups.

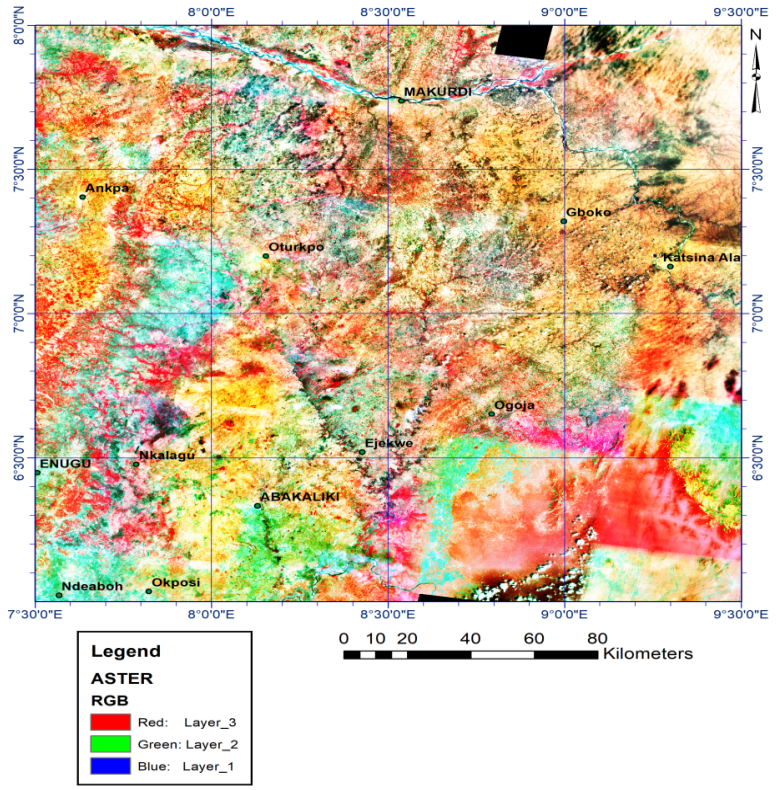

Figure 8: False Coloured Composite (321) of the study area.

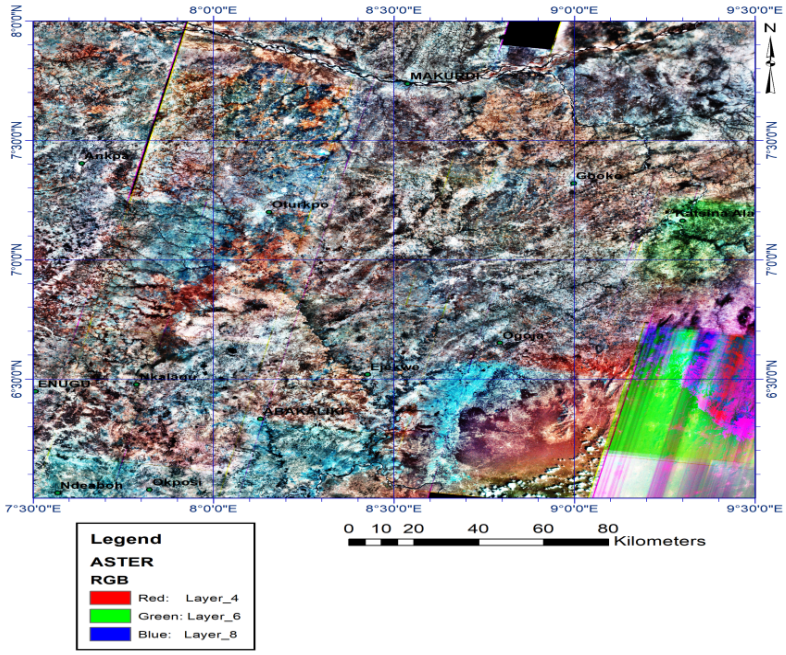

Figure 9: False Coloured Composite (468) of the study area.

The Band Ratio composite was created to differentiate the zones of alteration related to the ferric/ferrous minerals. Band Ratio of 4/2 is a good discriminator of the ferric oxides [56,57]. Aster band 4/2 was applied to highlight areas with abundant iron oxides bearing minerals. Figure 11 reveals areas where iron minerals (hematite, goethite, limonite, etc.) are abundantly shown in bright tones, the areas include Abakaliki, Ankpa, and Oturkpo.

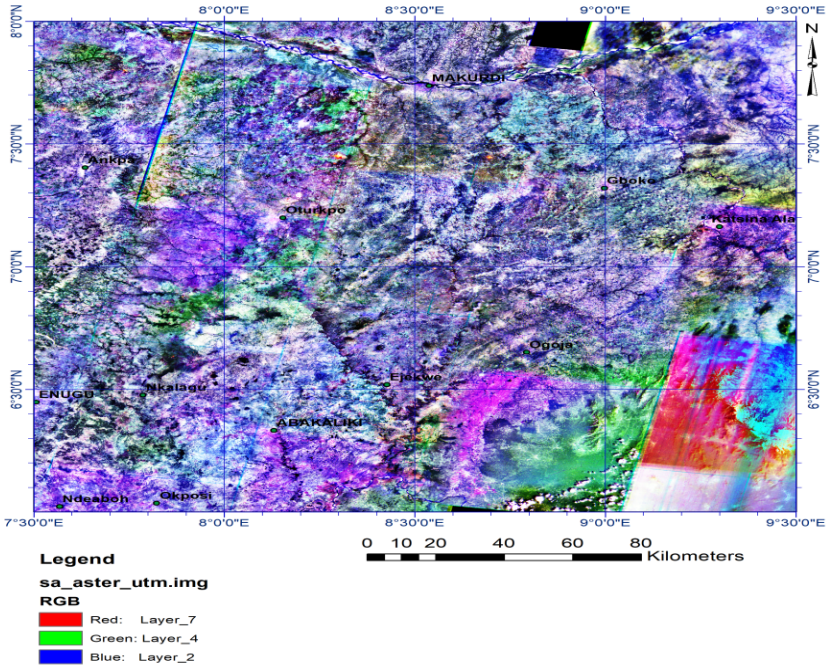

Figure 10: False Coloured Composite (742) of the study area.

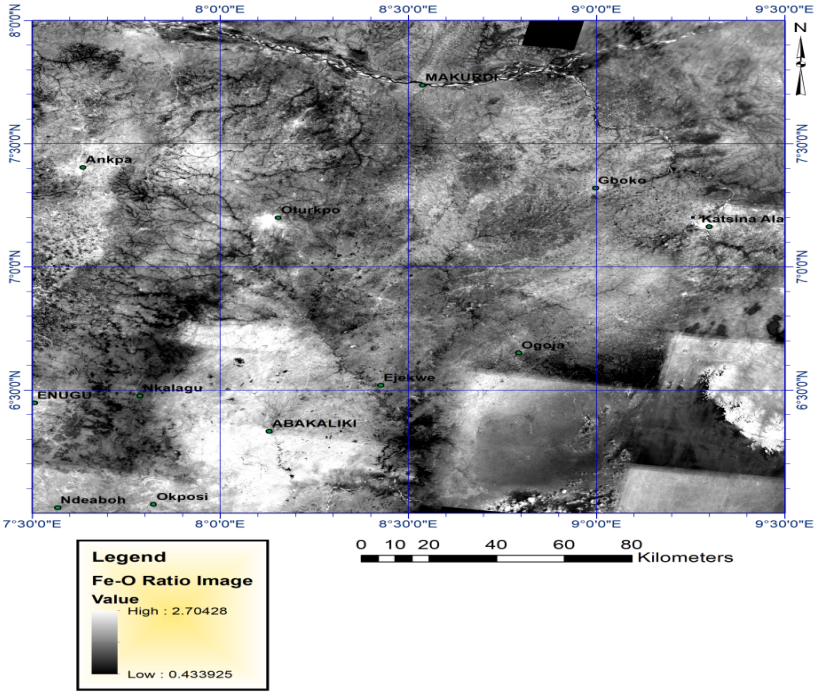

Figure 11: ASTER Band Ratio 4/2 image (Iron-rich minerals)

4.2 Discussion

The application of ASTER data as a convenient, time-saving, and effective tool for lineament and structural analysis was employed for this study. The pattern of drainage is dendritic and is an indication of lithology, structures, and differences in topography. Also, it indicates the presence of alluvial rocks which is a characteristic of the area and mostly sedimentary rocks. The dendritic design is observed around Makurdi, Katsina-ala, and Otukpo which describes regions having horizontal sedimentation or uniform crystalline rocks. Good knowledge of the characteristics of lineaments gives a clue about the regional tectonic history of an environment. A total of 983 lineaments were identified and delineated to generate a lineament map for the study area. The lineaments

extracted from ASTER imagery revealed the existence of two groups of linear features in NW-SE and NE-SW, with the dominant trend in the NE-SW orientation. The lineament trends corresponded to the position and direction of the paleo-tectonic fracture zones of the study area, which includes the St Paul's and Romanche Fracture Zones. Lineaments with long lateral extension revealed trends in the NE-SW, which suggest that the study area has undergone several phases of tectonic deformation. Lineaments in this area run parallel to each other and cross-cut each other, representing conjugate systems associated with wrench tectonics. The lineament density map in Figure 6 reveals a high concentration of lineaments around Enugu, Nkalagu, and Abakaliki. Areas having high density depicts a fault or fold development area, whereas a low-density area represents a relatively stable tectonic block. Ananaba and Ajakaiye [58], identified areas of high lineament density to be host to several minerals in Nigeria. The rose diagram (Figure 7) revealed the lineament trend orientation of E – W, N – S, NW – SE, and NE – SW having the dominant trend in NE – SW and corresponds to the major lineament trends of the study area. The N – S, NW-SE, and NNW – SSE orientation has been reported previously in the Pan-African basement by [59,60]. According to [61], the NE-SW trend is presumed to be a consequence of the pre-Albian rift of the African shield before the opening of the South Atlantic.

5. Conclusion

Structural analysis and interpretation of the study area were carried out using Advanced Spaceborne Thermal Emission and Reflection Radiometer (ASTER) satellite imagery. Several digital image processing techniques were applied to improve visual image interpretation for geological purposes, such as Lithological identification and lineament delineation. False colour composite images, RGB 321, RGB 468, and RGB 742 were generated and used to interpret geological structures. Band Ratio of 4/2 showed clear discrimination of areas with a high concentration of ferrous minerals. These areas appeared in bright pixels around hydrothermally altered areas. The Arc GIS V10.5 software was employed to carry out statistical analysis and lineament extraction within the study area. The result of the lineament analysis showed a large concentration of lineaments around the basement region. The lineaments run parallel to each other and cross-cut each. This is an indication that the area has undergone many tectonic activities. The Structural trends by the Rose diagram showed lineament trends of E – W, N – S, NW – SE, and NE – SW having the dominant trend in NE – SW corresponding to the major lineament trends of the study area. The map of lineament density, reveals areas having very high, high, moderate, low and very low lineament densities identified as 47,500m^2, 35,000m^2, 25,000m^2, 15,000m^2 and 5,000m^2 which represent 37.25%, 27.45%, 19.60%, 11.76% and 3.92% respectively. The dendritic drainage style is an indication of the difference in topography, structure, and lithology. It is also indicative of the geology of the area which consists mainly of sedimentary rocks overlying the basement. The NE-SW linear structures observed in the study area are believed to be the continental extension of pre-cretaceous oceanic fracture zones. The Charcot and Chain fracture zones run along the trough axis beneath the sedimentary cover [62,63]. The numerous lineaments in the study area make the region viable for mineral prospecting.

Declarations

Conflict of interest There is no conflict of interest to declare by the authors.
Funding No specific funding was received by the authors for this work.
Acknowledgement : The authors appreciate with thanks the support of the Management of the Federal University of Technology, Owerri, Nigeria, during the period of this study. We are also grateful to the anonymous reviewers for the meaningful suggestions and contributions, which greatly helped to improve the quality of this paper.

References

[1] Z. Adiri, A. El Harti, A. Jellouli, L. Maacha, and E. Bachaoui, Lithological mapping using Landsa OLI and Terra ASTER multispectral data in the Bas Draâ inlier, Moroccan Anti-Atlas. *Journal of Applied Remote Sensing*, 10(1) (2016) 016005 14.

[2] C. A. Alonso-Contes, Lineament mapping for groundwater exploration using remotely sensed imagery in a karst terrain: Rio Tanama and Rio de Arecibo basins in the northern karst of Puerto Rico. (2011)79.
[3] A. I. Opara, G. E. Odumosu, C. Z. Akaolisa, S. O. Onyekuru, T. T. Emberga, and N. N. Onu, Basement Depth Re-Evaluation and Structural Kinematic Analysis of Part of the Middle Benue Trough using High-Resolution Aeromagnetic Data. *Futo Journal Series*, 4(1) (2018) 409 – 436.
[4] S. A. Meshkani, B. Mehrabi, A. Yaghubpur, and M. Sadeghi, Recognition of the regional lineaments of Iran: Using geospatial data and their implications for exploration of metallic ore deposits. *Ore Geology Reviews,* 55(C) (2013) 48–63. doi.org/10.1016/j.oregeorev.2013.04.00.
[5] S. E. Ekwok, A. E. Akpan, D. E. Ebong, and O. E. Eze, Assessment of depth to magnetic sources using high resolution aeromagnetic data of some parts of the Lower Benue Trough and adjoining areas, Southeast Nigeria. *Advances in Space Research*, 67 (2021) 2104 – 2119.
[6] M. Abdullahi, and U. K. Singh, Basement geology derived from gravity anomalies beneath the Benue Trough of Nigeria. *Arabian Journal of Geosciences*, 11 (22) (2018) 694.
[7] O. K. Agagu, and C.I. Adighije, Tectonic and sedimentation framework of the lower Benue Trough, southeastern Nigeria. *Journal of African, Earth Science*, 1(3/4) (1983) 267–274.
[8] J. Benkhelil, The origin and evolution of the Cretaceous Benue Trough Nigeria. *Journal of African Earth Sciences*, 8 (1989) 251-282.
[9] O. U. Ekwueme, D. N. Obiora, E. A. Igwe and J. U. Abangwu, Study of aeromagnetic anomalies of Idah and Angba areas, north-central Nigeria, using high-resolution aeromagnetic data *Modeling Earth Systems and Environment*, 4 (2) (2018) 461–474.
[10] C. O. Ofoegbu, Interpretation of magnetic anomalies over the Lower and Middle Benue Trough of Nigeria. *Geophysical Journal Royal Astronomical Society*, 79 (1984) 813 – 823.
[11] B. E. Oguama, F. N. Okeke and D. N. Obiora, Mapping of subsurface structural features in some parts of Anambra Basin, Nigeria, using aeromagnetic data. *Modeling Earth Systems and environment*, 7 (2020)1623–1637. https://doi.org/10.1080/10106049.2020.1716395 .
[12] I. A. Omenikolo, T. T. Emberga and A. I. Opara, Basement depth re-valuation of anomalous magnetic bodies in the lower and middle Benue trough using Euler deconvolution and spectral inversion techniques. *World Journal of Advanced Research and Reviews*, 14(02) (2022) 129–145.
[13] A. I. Opara, Estimation of the Depth to Magnetic Basement in Part of the Dahomey Basin, Southwestern Nigeria. *Australian Journal of Basic and Applied Sciences*, 5(9) (2011) 335-343.
[14] A. I. Opara, R. A. Onyewuchi, A. O. Selemo, S. O. Onyekuru, B. O. Ubechu, T. T. Emberga, D. F. Ibim, and O. P. Nosiri, Structural and Tectonic Features of Ugep and Environs, Calabar Flank, Southeastern Nigeria: Evidences from aeromagnetic and Landsat-ETM data. *Mitteilungen, Klosterneuburg,* (2014) 64: 33-54.
[15] A. I. Opara, S. O. Oneyekuru, E. C. Mbagwu, T. T. Emberga, K. C. Ijeomah, and K. C. Nwokocha. Integrating Landsat – ETM and Aeromagnetic Data for Enhanced Structural Interpretation over Naraguta Area, North-Central Nigeria. *International J. of Scientific and Engineering Research*, 6(9) (2015)10.
[16] C. O. Ofoegbu, and K. M. Onuoha, Analysis of magnetic data over the Abakaliki Anticlinorium of the Lower Benue Trough, Nigeria. *Mar.Petrol. Geol*., 8 (1991) 174–183.
[17] A.G. Onwuemesi, One-dimensional spectral analysis of aeromagnetic anomalies and Curie depth isotherm in the Anambra Basin of Nigeria. *J. Geodyn*. 23(2) (1997) 95–107. https://doi.org/10.1016/S0264-3707(96)00028-2

[18] P. I. Olasehinde, P.C. Pal, and A. E. Annor, Aeromagnetic anomalies and structural lineament in the Nigerian Basement Complex. *Journal of African Earth Sciences*, 11(3/4) (1990) 351-355.
[19] I. A. Oha, K. M. Onuoha, A. N. Nwegbu, and A. U. Abba, Interpretation of high resolution aeromagnetic data over southern Benue Trough, southeastern Nigeria. *Journal of Earth System Science*,125(2) (2016) 369–385.
[20] M. A. Enoh, F. I. Okeke, and U. C. Okeke, Automatic lineaments mapping and extraction in relationship to natural hydrocarbon seepage in Ugwueme, South-Eastern Nigeria *Geodesy and Cartography,*47(1) (2021) 34–44.
[21] D. W. O'leary, J. D. Freidman, and H. A. Pohn, Lineament, linear, lineation: Some proposed new definitions for old terms; *Geol. Soc. Am. Bull*, 87 (1976) 1463–1469.
[22] M. Magowe, and J. R. Carr, Relationship between lineaments and groundwater occurrence in Western Botswana. *Ground Water*, 37(2) (1999) 282–286. https://doi.org/10.1111/j.1745-6584.1999.tb00985.x
[23] B. M. Moawad, Applications of remote sensing and geographic information system geomorphological studies: Safaga-El Quseir area, Red Sea, Egypt as an example VDM Verlag Dr Muller. 2008.
[24] Gupta RP. *Remote sensing geology* (2nd ed.). Springer. (2003) https://doi.org/10.1007/978-3-662-05283-9
[25] F. Sabins, Remote sensing: principles and interpretation (2nd ed.). Freeman. (1997)
[26] A. M. Casas, A.L. Cortés, A. Maestro, M. A.Soriano, A. Riaguas, and J. Bernal, LINDENS: A program for lineament length and density analysis. *Computers & Geosciences,* 26(9–10) (2000) 1011–1022. https://doi.org/10.1016/S0098-3004(00)00017-0
[27] A. I. Opara, A. C. Ekwe, C. N. Okereke, and O. P. Nosiri, Integrating airborne magnetic and Landsat data for geologic interpretation over part of the Benin basin, Nigeria. *The Pacific Journal of Science and Technology*, 13(1) (2012) 556–571.
[28] M. Pournamdary, M. Hashim, and B. A. Pour, Spectral transformation of ASTER and Landsat TM bands for lithological mapping of Soghan ophiolite complex, south Iran. *Advances in Space Research*, 54 (4) (2014b) 694–709.
[29] S. Gad, and T. Kusky, ASTER spectral rationing for lithological mapping in the Arabian-Nubian shield, the Neoproterozoic Wadi Kid area, Sinai, Egypt. Gondwana Research, 11 (2007) 326 – 335.
[30] S. D Khan, and N. F. Glenn, New strike-slip faults and litho-units mapped in Chitral (N. Pakistan) using field and ASTER data yield regionally significant results. *International Journal of Remote Sensing*, 27(20) (2006) 4495–4512. https://doi.org/10.1080/01431160600721830
[31] I. Di Tommaso, and N. Rubinstein, Hydrothermal alteration mapping using ASTER data in the Infiernillo porphyry deposit, Argentina. *Ore Geol. Rev.* 32 (2007) 275–290.
[32] A. Moghtaderi, F. Moore, and A. Mohammadzadeh, The application of advanced space-borne thermal emission and reflection (ASTER) radiometer data in the detection of alteration in the Chadormalu Paleo-crater, Bafq region, Central Iran. *Journal of Asian Earth Science*, 30 (2007) 238–252.
[33] A. B. Pour & M. Hashim, Identifying areas of high economic potential copper mineralization using ASTER data in the Urumieh-Dokhtar Volcanic Belt, Iran. *Adv. Sp. Res*. 49 (2012) 753–769
[34] A. B. Pour & M. Hashim, ASTER, ALI and Hyperion sensors data for lithological mapping and ore minerals exploration. *Springer Plus,* 3 (2014) 130. https://doi.org/10.1186/2193-1801-3-130

[35] M. Pournamdary, M. Hashim, and B. A. Pour, Application of ASTER and Landsat TM data for geological mapping of Esfandagheh ophiolite complex, southern Iran. *Resource Geol*., 64(3) (2014) 233-246.
[36] M. Pournamdary, M. Hashim, and B. A. Pour, Spectral transformation of ASTER and Landsat TM bands for lithological mapping of Soghan ophiolite complex, south Iran. *Advances in Space Research*, 54 (4) (2014b) 694–709.
[37] L. C. Rowan, and J. C. Mars, Lithologic mapping in the Mountain Pass, California area using Advanced Spaceborne Thermal Emission and Reflection Radiometer (ASTER) data. *Remote Sensing Environment*, 84 (2003) 350–366.
[38] M. Abdullahi, R. Kuma, and U. K. Singh, Magnetic basement depth from high- resolution aeromagnetic data of parts of lower and middle Benue Trough (Nigeria) using the scaling spectral method. *Journal of African, Earth Science*, 150 (2019) 337 – 345.
[39] C. O. Ajayi, and D. E. Ajakaiye, The origin and peculiarities of the Nigerian Benue Trough: another look from recent gravity data obtained from the Middle Benue. *Tectonophysics*, 8 (1981) 285-303.
[40] J. D. Carter, W. Barber, and E. A. Tait, The geology of parts of Adamawa, Bauchi and Bornu provinces in Northern Nigeria. *Bull. Geol. Surv. Nigeria*, (1963) 30.
[41] C. R. Cratchley, and G. P.Jones, An interpretation of the geology and gravity anomalies of the Benue valley, *Nigeria.Overseas Geol. Surv*. Geophysical Paper, (1965) 1.
[42] J. K. Ogunmola, E. A. Ayolabi, and S. B. Olobaniyi, Structural-depth analysis of the Yola Arm of the Upper Benue Trough of Nigeria using high-resolution aeromagnetic data, *Journal African Earth Science*, 124 (2016) 32–43.
[43] L. C. King, Outline and disruption of Gondwanaland. *Geol. Mag*., 87 (1950) 353-359.
[44] N. G. Obaje, Origin of the Benue Trough- A critical Review. In: Geology of Nigeria. C.A. Kogbe, (ed). Elizabeth Publishing Co., Lagos, Nigeria, (2004).
[45] K. Burke, T. Dessauvagie, and A. Whiteman, Opening of the Gulf of Guinea and Geological History of the Benue Depression and Niger Delta. *Nature Physical Science*, 233(1971) 51–55.
[46] R. A. Reyment, Aspects of Geology of Nigeria, Ibadan University Press, Ibadan Nigeria, (1965) 106.
[47] K. C. Short, and A. J. Stauble, Outline geology of the Niger Delta. *American Association of Petroleum Geologists. Bulletin*, 51 (1967) 761-77.
[48] S. O. Nwachukwu, Approximate geothermal gradients in Niger Delta sedimentary basin. *America Association of Petroleum Geologists*. Bulletin, 60(7) (1972) 1073 – 1077.
[49] M. A. Olade, Evolution of Nigeria's Benue Trough (Aulacogen): a tectonic model. *Geol.Mag.*, 112 (1975) 575-581.
[50] H. Fujisada, M. Urai, and A. Iwasaki,Technical methodology for ASTER global DEM. IEEE Trans. *Geoscience Remote Sensing*, 50 (10) (2012) 3725–3736.
[51] J. Inzana, T. Kusky, G. Higgs, and R. Tucker, Supervised classifications of Landsat TM band ratio images and Landsat TM band ratio images with radar for geological interpretations of central Madagascar. *Journal of African, Earth Science*, 37 (2003) 59-72.
[52] A. C. Umeji, The Precambrian of part of the SE Nigeria: A magmatic and Tectonic study. In : P.O. Oluyide PO W.C. Mbonu WC. Oguzie AE. Egbuniwe IG. Ajibade AC, an Umeji AC (Eds.), Precambrian Geology of Nigeria, Geological Survey of Nigeria, (1988) 69-75.
[53] J. D. Fairhead, C. M. Green, S. M. Masterton, and R. Guiraud, The role of plate tectonics

that inferred stress changes and stratigraphic unconformities have on the evolution of the West and Central African rift system and the Atlantic continental margins. *Tectonophysics*, 594 (2013) 118-127.
[54] C. Gaina, H. T. Trond, D. J. J. Van Hinsbergen, M. Sergei, S. C. Werner, and C. Labails, The African Plate: a history of oceanic crust accretion and subduction since the Jurassic. *Tectonophysics*, 604 (2013) 4–25.
[55] C. O. Ofoegbu, An Aeromagnetic Study of Part of the Upper Benue Trough, Nigeria. *Journal of African Earth Science*, 7 (1988) 77- 90.
[56] T. Cudahy, Satellite ASTER *Geoscience Product Notes Western Australia,* 2(1) (2012): 1–23.
[57] A. Kalinowski, and S. Oliver, ASTER Mineral Index Processing Manual Remote Sensing Applications, *Geoscience,* Australia. (2004).
[58] S. E. Ananaba, and D. E. Ajakaiye, Evidence of tectonic control of mineralization of Nigeria from lineament density analysis: A Landsat study; *International Journal of Remote Sensing*, 8(10) (1987) 1445-1453
[59] A. E. Edet, C. S. Teme, C. S. Okereke, and E. O. Esu, Lineament analysis for groundwater exploration in Precambrian Oban Massif and Obudu Plateau, SE Nigeria. *Journal of Mining and Geology*, 30 (1) (1994) 87-95.
[60] P. O. Oluyide, "Structural Trends in the Nigerian Basement Complex. Precambrian Geology of Nigeria," *Geological Survey of Nigeria Publication*, Kaduna, 1988; 93-98.
[61] A. B. Uzuakpunwa, The Abakaliki pyroclastics-eastern Nigeria: New age and tectonic implications, *Geological Magazine* III, (1974) 65-70.
[62] S. E. Ananaba, Dam sites and crustal mega-lineaments in Nigeria. *ITC Journal*, 1 (1991) 26-29.
[63] C. N. Okereke, and S. E. Ananaba, Deep crustal Lineament inferred from aeromagnetic anomalies over the Niger Delta, Nigeria. *Journal of Mining and Geology*, 42(2) (2006) 127-131.